Ultrathin, Ultrasmooth Gold Layer on Dielectrics without the Use of Additional Metallic Adhesion Layers

Lorenzo Leandro,[†] Radu Malureanu,*,[†] Noemi Rozlosnik,[‡] and Andrei Lavrinenko[†]

[†]Department of Photonics Engineering and [‡]Technical University of Denmark, Oersteds Plads, Building 345v, Room 178, DK-2800 Kongens Lyngby, Denmark

S *Supporting Information*

ABSTRACT: With advances in the plasmonics and metamaterials research field, it has become more and more important to fabricate thin and smooth Au metal films in a reliable way. Here, by thin films we mean that their average height is below 10 nm and their average roughness is below 5% of the total thickness. In this article, we investigated the use of amino- and mercaptosilanes to increase the adhesion of Au on Si wafers, thus obtaining a smooth and thin layer. This method does not include the use of other metals to improve the adhesion of gold, like Ti or Cr, since they would reduce the optical characteristics of the structure. Our results show that layers having 6 nm thickness and below 0.3 nm roughness can be reproducibly obtained using aminosilanes. Layers having a nominal thickness of 5 nm have a yield of 58%; thus, this thickness is the limit for the process that we investigated.

KEYWORDS: *6 nm gold complete layer, nonmetallic adhesion layer, ultrasmooth, plasmonics, hyperbolic metamaterials, aminosilane*

1. INTRODUCTION

The possibility of having 10 nm layers of metal on a substrate is a research topic widely studied.[1−3] It would be useful in several applications such as of plasmonic waveguides[4] or hyperbolic metamaterials.[5] An ultrathin, ultrasmooth metal layer on dielectrics can allow us to increase the band of use of hyperbolic metamaterials and can highly increase the propagation length of surface plasmon polaritons (SPPs) through the structure,[6,7] thus bringing this field closer to the large-scale implementation level. The main parameters to be considered for improving the functionality are roughness, thickness, and optical proprieties of the metal.

The objective of this work is to investigate the possibility of improving the adhesion of gold on silicon oxide in order to decrease the thickness of the layer of metal on the dielectric substrate. The deposition of Au on silicon or oxidized substrates follows the Volmer−Weber growth mode, thus creating a perfect layer only over a certain thickness through clusters that connect to each other. A reduction of this lower limit for the thickness can be achieved by improving the adhesion between Au and the substrate. The current value for this limit is between 10 and 15 nm.[8,9] The usual approach for adhesion improvement is using Ti or Cr layers. The addition of these metals significantly deteriorates the optical properties of the layer, and this effect is more pronounced for thin films since the ratio between Au and the other metal increases.[10] In this work we analyze a way to increase the adhesion of gold that does not include the use of other metals.

This study analyzes the adhesion given by various organosilane chemicals.[11−13] These organosilanes bind to the silicon surface by hydrolysis and condensation of silane creating covalent bonds on the surface. Linked to silane, a carbon chain connects the substrate with a radical. Different radicals were evaluated, and their quality as an adhesion promoter for gold was analyzed. Furthermore, we studied the deposition of various thicknesses of gold with different deposition rates. We made the latter investigation in order to establish the lower limit for the thickness. The layer quality was investigated using scanning electron microscopy (SEM), atomic force microscopy (AFM), and four-point probe techniques. Although there are tests[14] showing improvement of gold adhesion on silica by using aminosilanes, the limits of Au deposition and a comparison with mercaptosilanes have not been yet investigated to our knowledge.

2. METHODS

We used Czochralski-based epitaxial (CZ-EPI) 4 in. silicon wafers from TOPSIL for our experiments. The wafers have a resistivity between 1 and 20 Ω cm, and they are phosphorus doped. The crystal orientation is {100}. The wafers were not treated before silane deposition; thus, they all have ca. 5 nm native oxide layer. After surface treatment (described below), the wafers were cleaved in 1.5 × 1.5 cm pieces for gold deposition.

The surface treatment consists in immersing a silicon wafer in a solution of 95% of Isopropyl Alcohol, 2.5% of water, and 2.5% of silane for 3 h.[14−17] The surface treatment took place in a fumehood in a class 1000 cleanroom with a controlled temperature of 22° ± 2° and humidity of 44% ± 2%. The samples were immersed in 100 mL of

Figure 1. Images taken using the SEM of samples on which 6 nm of gold has been deposited with a rate of 9.5 Å/s on Si (a) and after a treatment with (3-(2-aminoethylamino)propyl)trimethoxysilane (b), (3-mercaptopropyl)trimethoxysilane (c), (3-aminopropyl)triethoxysilane (d), and (3-aminopropyl)trimethoxysilane (e).

freshly prepared solution and covered in order to limit the polymerization process that takes place at the air/solution interface.

We performed several tests to find the optimum immersion time. Less than 3 h would not allow the chemical to react properly with the surface, inducing less adhesion promotion and thus a rougher metal layer (See Supporting Information, Figure 1). More time would not help to improve the adhesion (see Supporting Information, Figure 2) but will increase the amount of polymerized silane, thus adding difficulties in obtaining a clean surface. For this reason, we recommend not leaving the wafer in solution for more than 3 h and also to use more solution than needed to just cover the whole wafer. Indeed, the polymerized silane seems to accumulate in the upper part of the liquid; thus, having more mixture and keeping the wafer in the lower part of the beaker will result in a cleaner wafer.

We tested four different chemicals, all purchased from Sigma-Aldrich:

- (3-mercaptopropyl)trimethoxysilane, $HS(CH_2)_3Si(OCH_3)_3$, 95%;
- (3-(2-aminoethylamino)propyl)trimethoxysilane, $(CH_3O)_3Si(CH_2)_3NHCH_2\,NH_2$, 80%;
- (3-aminopropyl)triethoxysilane, $H_2N(CH_2)_3Si(OC_2H_5)_3$, 99%;
- (3-aminopropyl)trimethoxysilane, $H_2N(CH_2)_3Si(OCH_3)_3$, 97%.

For reference, a standard silicon sample was used.

The deposition of gold was made after chemical treatment using an E-beam evaporation system (deposition pressure $2-4 \times 10^{-6}$ Pa). The Au used has a purity of 99.999% and was acquired from Kurt J. Lesker(r). We made several tests to understand how the deposition
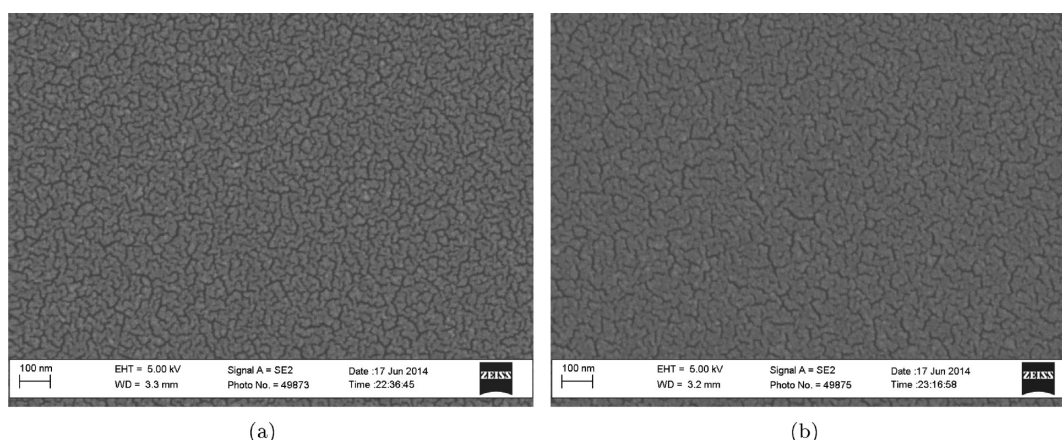
Figure 2. Images taken using the SEM of samples on which 5 nm of gold has been deposited with a rate of (a) 5 and (b) 10 Å/s after treatment with (3-aminopropyl)trimethoxysilane on a silicon substrate.

rate affects the surface quality and so the minimum thickness that creates a complete layer. We focused on maintaining the deposition rate as stable as possible, and we compared the resultant surface only if made during the same process to reduce the impact of the uncertainty in the deposition. Thicknesses from 4 to 10 nm and deposition rates from 5 to 13 Å/s were evaluated.

We investigated the surfaces after gold deposition by SEM in order to see the quality and completeness of the deposited layers. All images presented show the typical surface of the sample, with a EHT of 5 kV, a magnification of 175 000, and a working distance between 2 and 4 mm. Roughness and thickness measurements were done using AFM. The metal thickness measure comes with higher uncertainties due to the length and positioning of silane on the surface. The sheet resistance was measured by the four-point probe method. Each sample was measured 10 times in different areas, and the average and standard deviation of the sheet resistance were calculated.

3. RESULTS

A first test was performed for deciding the best silane to be used. From the images shown in Figure 1, with 6 nm of gold deposited at 9.5 Å/s we were able to see an improvement of the adhesion of the metal on the substrate for all four silanes used, compared with the untreated silicon case. In the case of (3-(2-aminoethylamino)propyl)trimethoxysilane, although the layer is better than the untreated wafer, it is worse that the other chemicals (Figure 1). This is probably due to the presence of two amino groups, one of which is placed in the middle of the carbon chain.

On the other hand, complete layers are shown on the (3-aminopropyl)triethoxysilane- and (3-aminopropyl)-trimethoxysilane-treated samples. In order to quantify the layer quality, we postprocessed the images and estimated the percentage of voids area with respect to the total image. We calculated this area by cropping the image such that only the layer was shown and then applied a threshold to define where the voids are. The threshold level was calculated for each image as 25% of the dynamic range from the minimum level. In the case of untreated sample (Figure 1a), the metal filling fraction was 91%. The (3-(2-aminoethylamino)propyl)trimethoxysilane showed a small improvement, having a filling fraction of 94%, while all other tests showed more than 95%. Out of these last three, the (3-mercaptopropyl)trimethoxysilane had the lowest filing fraction of 95% while the amino-based layers produced a coverage of above 97%. We should add that these estimations have a relatively big margin of error due to the intrinsic noise present in the image; thus, we considered significant variation

only if the difference was above 1%. Also, we consider a full layer if the metal filling fraction is above 97%. We kept the aminosilanes for further analysis.

We tried to differentiate between the two aminosilanes by depositing 4 nm layers. Still, we could not observe a statistical difference between the filling fraction of Au using one or another of the aminosilanes (see Supporting Information, Figure 3). When testing layers of 8 nm nominal thickness, we obtained complete coverage for (3-mercaptopropyl)-trimethoxysilane, (3-aminopropyl)triethoxysilane, and (3-aminopropyl)trimethoxysilane. The wafer treated with (3-(2-aminoethylamino)propyl)trimethoxysilane had 98% filling fraction showing a significant improvement with the 6 nm case. The untreated sample had 93% filling fraction, thus only marginally better than the 6 nm case, as expected (see Supporting Information, Figure 4). We decided to use (3-aminopropyl)trimethoxysilane for the last analysis, since it is more chemically stable.

An initial check of the surface adhesion was made by comparing the contact angle of water on the (3-aminopropyl)-trimethoxysilane-treated wafer with the one on the untreated Si wafer. We used a Krüss DSA100 drop shape analyzer dispensing 2 µL of water at a rate of 30 µL/min. In the case of the untreated Si, the contact angle was 32.1° ± 0.2°, as expected also from the literature.[18] We would like to stress that the native silicon was not removed during the procedure; thus, the measured contact angle is closer to the one of silica than to the one of silicon. The contact angle on the treated sample was 10.3° ± 0.48°, showing a significant increase in the hydrophilicity of the surface.

Analyzing surfaces treated with the same chemicals but with gold deposited at different rates, between 5 and 13 Å/s (maximum rate for our machine), we were able to prove that increasing the deposition rate the surface quality also increases. This effect is shown in Figure 2, where we can see two samples, treated with the same chemical and covered by gold at different deposition rates. Using the same technique for determining the metal filling fraction, we reached 93% for the sample deposited at 5 Å/s and 95% for the one deposited at 10 Å/s.

To be noted, the deposited adhesion promoter is reactive; thus, Au deposition should be done as soon as possible after surface treatment. We had a huge decrease of the adhesion promotion for gold deposited after 3 or 5 days after treatment,

compared with the ones deposited just after or shortly after surface treatment.

A sample on which 6 nm of gold was deposited at a rate of 9.5 Å/s was used for roughness analysis. The results in Figure 3 show a surface roughness below 0.26 nm with an RMS of 0.19 nm.
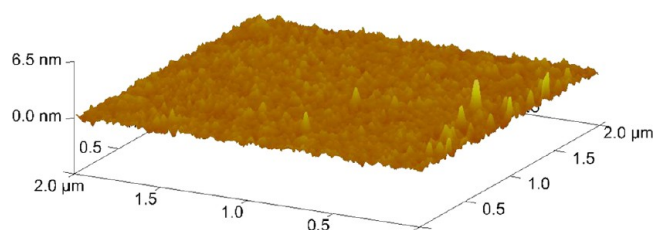
Figure 3. Pictures taken using the AFM of a sample on which 6 nm of gold was deposited with a rate of 9.5 Å/s after treatment with (3-aminopropyl)trimethoxysilane.

Further analysis was made using (3-aminopropyl)-trimethoxysilane, depositing 5 nm of gold with a rate of 13 Å/s on four sets of four samples each. For each set we ran a deposition process using always the same parameters. The resultant images show that 5 nm thickness can be considered as the "critical point" for gold deposition.

We see, in the example in Figure 4, that a deposition of 5 nm of gold cannot create a complete layer in a reproducible manner. We found that the quality of the surfaces is good enough to be considered a layer in about 58% of the cases: 7 out of 12 samples showed the surface covered by a continuous layer of gold. In the same time, for a nominally 6 nm layer, we obtained 100% reproducibility: all our samples had a continuous layer after deposition. This allows us to define 6 nm as the minimum thickness where we can reproducibly obtain a complete layer, and as such 5 nm is the critical thickness. We also performed a thorough investigation of 4 nm nominal thickness layers (see Supporting Information, Figure 5). In this case, none of our samples had a complete layer of gold deposited on.

Due to the combination of a small thickness and fast deposition rate, we have uncertainties in the deposited thickness. Our AFM measurements show a total thickness between 6.0 and 6.8 nm for a 5 nm deposition. Considering that the silane carbon chains have a length of 0.8 nm,[19] we have a discrepancy between 0.2 and 1 nm. We believe this discrepancy to arise from the uncertainties on the deposited thickness as well as from the layer roughness. As shown in Table 1, we saw high roughness values (22 nm) for the 4 nm thick gold sample, with a maximum height difference of 190 nm. Much lower values for the other samples mean that the roughness decreases rapidly, increasing the thickness from 4 to 5 nm, showing that the surface quality improves very fast. Also, in Table 1 are shown the average resistivity and its standard deviation calculated from 10 measurements for each sample. The resistivity values have to be compared with the ones estimated from the Drude model for thin gold films. On the basis of ref 20 we calculated the gold resistivity in the long wavelength limit. Thus, for $\lambda \rightarrow \infty$, the resistivity becomes

$$\rho = \frac{\Gamma(r)}{w_p^2 \varepsilon_0}$$

where $\Gamma(r)$ is the size-dependent damping frequency and ω_p is the plasma frequency. To be noted that for bulk gold, when $r \rightarrow \infty$, $\Gamma(r)$ becomes Γ_-. In this case, the bulk gold resistivity is 19.5 nΩ m (for further information about the notations refer to[20]). This value is underestimated with respect to the one found in the literature of 24.4 nΩ m;[21] thus, we believe that the calculated values of resistivity might also be different from the real ones. This fact might easily explain the discrepancy in Table 1 where the measured resistivity value is smaller than the estimated one in the case of the 6 nm thick layer.

We would like to mention that a complete description of the growth method is not the focus of this paper. Still, in the following and based on the available data, we can provide a basic description of our understanding of the growth method. In the case of the 4 nm layer, the estimated resistivity is almost 10 times lower than the average one. This discrepancy is a clear indication that the Drude model we are using, assuming there is a continuous layer, is not working anymore. Together with the measured roughness, which is 4.5 times higher than the nominal thickness, the maximum height of almost 50 times bigger and the huge difference with respect to the Drude model is a strong indication that until this stage the Au follows a Volmer−Weber growth as described in ref 22. In between the 4

(a)   (b)
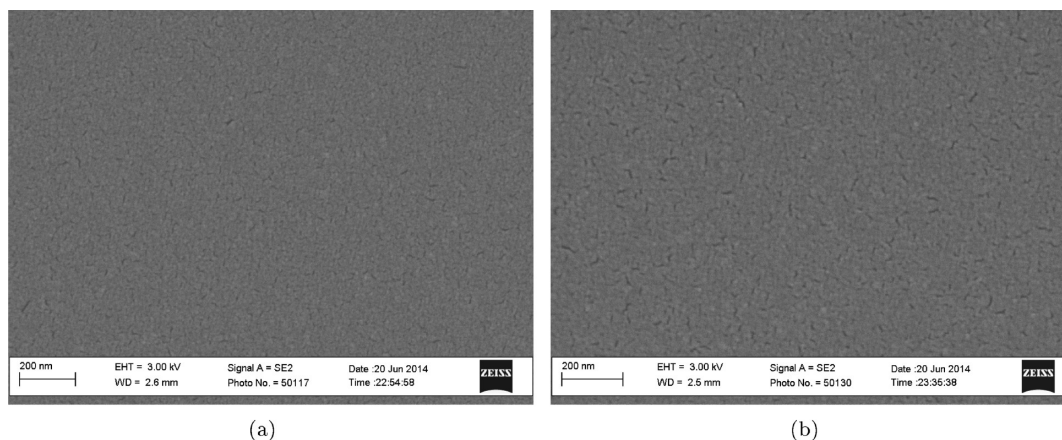
Figure 4. Pictures taken using the SEM of two samples, made in different processes, on which 5 nm of gold has been deposited with a rate of 13 Å/s using the Alcatel SCM 600 E-beam and sputtering deposition system after treatment with (3-aminopropyl)trimethoxysilane: (a) sample n.2, set 1, considered a layer; (b) sample n.2, set 2, not considered a layer.

Table 1. Estimated Resistivity for Thin Gold Films Calculated from Ref 20, Average Resistivity and Its Standard Deviation Calculated from 10 Measurements for Each Sample Made with a Four-Probe Method, Roughness, Its Root Mean Square, and Its Peak-to-Valley Maximum Value[a]

height [nm]	estimated resistivity [nΩ m]	average resistivity [nΩ m]	standard deviation [nΩ m]	roughness [nm]	RMS [nm]	maximum height [nm]	filling fraction [%]
4	219.7	1840.8	74.4	17.4	22	190	95
5	179.6	326.4	14.0	0.60	0.75	6.89	95−98
6	152.9	106.9	2.22	0.19	0.26	4.55	98

[a]The considered samples are covered by 4, 5, and 6 nm of gold, respectively, deposited at 9.5 Å/s.

and 5 nm nominal thickness there is a clear change in the growth mechanism. We suspect that the cluster growth that is predominant until this thickness changes character and a growth model similar to a layer-by-layer one takes place.[23] In the same time, the Au atoms are very mobile, and once the clusters connect at a nominal thickness in between 4 and 5 nm, they will tend to rearrange themselves in a more layered fashion. Further analysis as described in refs 24 and 25 may confirm this understanding.

4. CONCLUSION

We were able to reproducibly deposit a complete 6 nm thick gold layer on a silica surface. The adhesion was improved by treating the surface with (3-aminopropyl)trimethoxysilane. Different silanes were compared with an untreated silicon sample, and they proved to act as adhesion promoters. Aminosilanes showed better results compared with mercaptosilanes. We showed that the increase in deposition rate improves the surface quality and lowers the minimum thickness limit. The thickness measurements, together with the surface quality check and the four-probe resistivity measurements, convincingly demonstrated that it is possible to deposit a good-quality gold layer of thickness as low as 5 nm. Finally, roughness measurements of the 6 nm thick layer showed very low average roughness below 0.2 nm with 0.3 nm RMS. Although further investigation is needed to determine the growth method, we believe it to be a combination of the Volmer−Weber method until a nominal thickness of 4 nm and a layer-by-layer growth method with rearranging of Au atoms above this thickness.

■ ASSOCIATED CONTENT

Ⓢ Supporting Information

SEM images of Au deposition using different surface treatments and aiming at various thicknesses. This material is available free of charge via the Internet at http://pubs.acs.org.

■ AUTHOR INFORMATION

Corresponding Author
*E-mail: rmal@fotonik.dtu.dk.
Notes
The authors declare no competing financial interest.

■ REFERENCES

(1) Formica, N.; Ghosh, D. S.; Carrilero, A.; Chen, T. L.; Simpson, R. E.; Pruneri, V. Ultrastable and Atomically Smooth Ultrathin Silver Films Grown on a Copper Seed Layer. *ACS Appl. Mater. Interfaces* **2013**, *5*, 3048−3053.

(2) Smith, D. R.; Padilla, W. J.; Vier, D. C.; Nemat-Nasser, S. C.; Schultz, S. Composite Medium with Simultaneously Negative Permeability and Permittivity. *Phys. Rev. Lett.* **2000**, *84*, 4184−4187.

(3) Fang, N.; Lee, H.; Sun, C.; Zhang, X. Sub-Diffraction-Limited Optical Imaging with a Silver Superlens. *Science* **2005**, *308*, 534−537.

(4) Park, J. H.; Ambwani, P.; Manno, M.; Lindquist, N. C.; Nagpal, P.; Oh, S.-H.; Leighton, C.; Norris, D. J. Single-Crystalline Silver Films for Plasmonics. *Adv. Mater.* **2012**, *24*, 3988−3992.

(5) Kidwai, O.; Zhukovsky, S. V.; Sipe, J. E. Effective-medium Approach to Planar Multilayer Hyperbolic Metamaterials: Strengths and Limitations. *Phys. Rev. A: At., Mol., Opt. Phys.* **2012**, *85*, 053842.

(6) Nagpal, P.; Lindquist, N. C.; Oh, S. H.; Norris, D. J. Ultrasmooth Patterned Metals for Plasmonics and Metamaterials. *Science* **2009**, *325*, 594−597.

(7) Sarid, D. Long-range Surface-plasma Waves on Very Thin Metal-Films. *Phys. Rev. Lett.* **1981**, *47*, 1927−1930.

(8) Hammiche, A.; Webb, R. P.; Wilson, I. H. A Scanning Tunnelling Microscopy Study of Thin Gold Films Evaporated on Silicon. *Vacuum* **1994**, *45*, 569−573.

(9) Malinský, P.; Slepička, P.; Hnatowicz, V.; Svorčík, V. Early Stages of Growth of Gold Layers Sputter Deposited on Glass and Silicon Substrates. *Nanoscale Res. Lett.* **2012**, *7*, 241.

(10) Habteyes, T. G.; Dhuey, S.; Wood, E.; Gargas, D.; Cabrini, S.; Schuck, P. J.; Alivisatos, A. P.; Leone, S. R. Metallic Adhesion Layer Induced Plasmon Damping and Molecular Linker as a Nondamping Alternative. *ACS Nano* **2012**, *6*, 5702−5709.

(11) Gentle, T.; Schmidt, R.; Naasz, B.; Gellman, A.; Gentle, T. Organofunctional Silanes as Adhesion Promoters: Direct Characterization of the Polymer Silane Interphase. *J. Adhes. Sci. Technol.* **1992**, *6*, 307−316.

(12) Polniaszek, M.; Schaufelberger, R. Improving Adhesives with Silane Adhesion Promoters. *Adhes. Age* **1968**, *11*, 25−27.

(13) Doron, A.; Katz, E.; Willner, I. Organization of Au Colloids as Monolayer Films onto ITO Glass Surfaces: Application of the Metal Colloid Films as Base Interfaces to Construct Redox-active Monolayers. *Langmuir* **1995**, *11*, 1313−1317.

(14) Petri, D.; Wenz, G.; Schunk, P.; Schimmel, T. An Improved Method for the Assembly of Amino-terminated Monolayers on SiO2 and the Vapor Deposition of Gold Layers. *Langmuir* **1999**, *15*, 4520−4523.

(15) Ulman, A. Formation and Structure of Self-Assembled Monolayers. *Chem. Rev.* **1996**, *96*, 1533−1554.

(16) Madsen, H. B.; Arboe-Andersen, H. M.; Rozlosnik, N.; Madsen, F.; Ifversen, P.; Kasimova, M. R.; Nielsen, H. M. r. Investigation of the Interaction Between Modified ISCOMs and Stratum Corneum Lipid Model Systems. *Biochim. Biophys. Acta* **2010**, *1798*, 1779−89.

(17) Howarter, J. A.; Youngblood, J. P. Optimization of Silica Silanization by 3-aminopropyltriethoxysilane. *Langmuir* **2006**, *22*, 11142−11147.

(18) Williams, R.; Goodman, A. M. Wetting of Thin Layers of SiO2 by Water. *Appl. Phys. Lett.* **1974**, *25*, 531−532.

(19) Moon, J. H.; Shin, J. W.; Kim, S. Y.; Park, J. W. Formation of Uniform Aminosilane Thin Layers: An Imine Formation To Measure Relative Surface Density of the Amine Group. *Langmuir* **1996**, *12*, 4621−4624.

(20) Gordon, J. A.; Ziolkowski, R. W. The Design and Simulated Performance of a Coated Nano-particle Laser. *Opt. Express* **2007**, *15*, 2622−2653.

(21) Serway, R., Jewett, J. *Principles of Physics: A Calculus-Based Text*; Cengage Learning: Boston, MA, 2005.

(22) Schwartzkopf, M.; et al. From Atoms to Layers: In Situ Gold Cluster Growth Kinetics During Sputter Deposition. *Nanoscale* **2013**, *5*, 5053−62.

(23) Yu, S.; Santoro, G.; Sarkar, K.; Dicke, B.; Wessels, P.; Bommel, S.; Döhrmann, R.; Perlich, J.; Kuhlmann, M.; Metwalli, E.; Risch, J. F. H.; Schwartzkopf, M.; Drescher, M.; Müller-Buschbaum, P.; Roth, S. V. Formation of Al Nanostructures on Alq3: An in Situ Grazing Incidence Small Angle X-ray Scattering Study during Radio Frequency Sputter Deposition. *J. Phys. Chem. Lett.* **2013**, *4*, 3170−3175.

(24) Kaune, G.; Ruderer, M. A.; Metwalli, E.; Wang, W.; Couet, S.; Schlage, K.; Röhlsberger, R.; Roth, S. V.; Müller-Buschbaum, P. In Situ GISAXS Study of Gold Film Growth on Conducting Polymer Films. *ACS Appl. Mater. Interfaces* **2009**, *1*, 353−360.

(25) Roth, S. V.; Walter, H.; Burghammer, M.; Riekel, C.; Lengeler, B.; Schroer, C.; Kuhlmann, M.; Walther, T.; Sehrbrock, A.; Domnick, R.; Müller-Buschbaum, P. Combinatorial Investigation of The Isolated Nanoparticle to Coalescent Layer Transition in A Gradient Sputtered Gold Nanoparticle Layer on Top of Polystyrene. *Appl. Phys. Lett.* **2006**, *88*, 21910−1−3.

(26) Scarpettini, A. F.; Bragas, A. V. Coverage and Aggregation of Gold Nanoparticles on Silanized Glasses. *Langmuir* **2010**, *26*, 15948− 15953.

(27) Yang, J.; Ichii, T.; Murase, K.; Sugimura, H. Site-Selective Assembly and Reorganization of Gold Nanoparticles along Amino-silane-Covered Nano lines Prepared on Indium-Tin Oxide. *Langmuir* **2012**, *28*, 7579−7584.

(28) Yamashiro, K.; Murase, K.; Ichii, T.; Mo, S.; Sugimura, H. Photochemical Assembly of Gold Nanoparticle Arrays Covalently Attached to Silicon Surface Assisted by Localized Plasmon in the Nanoparticles. *J. Phys. Chem. C* **2013**, *117*, 2480−2485.

(29) Chen, C.-F.; Tzeng, S.-D.; Lin, M.-H.; Gwo, S. Electrostatic Assembly of Gold Colloidal Nanoparticles on Organosilane Mono-layers Patterned by Microcontact Electrochemical Conversion. *Langmuir* **2006**, *22*, 7819−7824.